Carrier-induced optical bistability in silicon ring resonators

Qianfan Xu and Michal Lipson

School of Electrical and Computer Engineering, Cornell University, 411 Phillips Hall, Ithaca, New York 14853

Received July 19, 2005; accepted September 15, 2005

We demonstrate optical bistability in a micrometer-sized silicon ring resonator based on the free-carrier dispersion effect in silicon. We measure the transfer function of the resonator showing a hysteresis loop with an input optical power of less than 10 mW. The influence of the thermal optical effect, which is minimized in the experiment by use of nanosecond pulses, is evaluated theoretically. Applications include sequential logic operations for all-optical routing. © 2006 Optical Society of America

OCIS codes: 130.4310, 190.1450.

Optical integration in silicon has shown great potential because of its compatibility with microelectronics. Active optical devices have been demonstrated in silicon.[1–4] We have shown both all-optical[4] and electro-optical modulators,[3] using silicon ring resonators based on the free-carrier dispersion effect in silicon. Combinational logic has been realized based on all-optical switching with III–V semiconductor ring resonators.[5,6] However, applications such as all-optical routing require the state of a switch to be controlled by previous information (the header of a packet, for example), and therefore combinational logic is not sufficient. For these applications, the bistability effect needs to be demonstrated so that sequential logic elements can be built. In silicon, optical bistability due to the thermal optical effect has been observed.[7] However, the thermal effect is relatively slow, with a microsecond transition time. Recently, optical bistability based on the carrier effect was also demonstrated by use of photonic crystal cavities.[8] In this Letter we show experimental measurement of the carrier-induced optical bistability effect in a silicon ring resonator with a nanosecond transition time. Using a high-quality-factor ring resonator, we obtain a bistability hysteresis loop with less than 10 mW of input optical power. The influence of the thermal effect on the carrier-induced bistability effect is also analyzed.

The structure used in the experiment consists of a silicon ring coupled to a straight waveguide, as shown in the inset of Fig. 1. It is fabricated on a silicon-on-insulator substrate with a 3 μm buried oxide layer by the process described in Ref. 9. The waveguides that form the structure have a width of 450 nm and a height of 250 nm. The radius of the ring is $R=5$ μm. Nanotapers are used at both ends of the waveguide to expand the mode diameter to ~ 5 μm, ensuring low-loss coupling to optical fibers.[9] At the input side, light is coupled through a tapered lens fiber to the nanotaper. At the output side, light is coupled into fiber from the nanotaper through a lens and a collimator. The fiber-to-fiber insertion loss for the quasi-TE mode (dominant electric field parallel to the substrate) is measured to be 10.4 dB, which includes an input coupling loss of 2.7 ± 0.2 dB, a waveguide transmission loss of 4.1 ± 0.1 dB (8 mm long waveguide with a 5.1 ± 0.1 dB/cm attenuation coefficient), and an output coupling loss of 3.6 ± 0.4 dB. The waveguide transmission loss was extracted from the insertion losses of waveguides of different lengths.

Figure 1 shows the transmission spectrum about the resonant wavelength of $\lambda_0=1532.85$ nm for the quasi-TE mode. The spectrum shows a 14 dB drop of transmission at the resonant wavelength when the light in the waveguide is coupled to the ring and is lost from scattering at the sidewalls of the ring. The full width at half-maximum bandwidth of the resonance is $\Delta\lambda_{FWHM}=0.11$ nm, corresponding to a quality factor, defined as $Q=\lambda_0/\Delta\lambda_{FWHM}$, of 14,000. The TM mode has different resonant wavelengths and different values of Q.

The bistability effect is based on the carrier generation induced by two-photon absorption[10] (TPA) in the ring resonator. The generated free carriers induce a decrease of refractive index of silicon and cause a blueshift of the resonant spectrum of the ring resonator. If the wavelength of the optical pulses is shorter than the resonance when no free carriers are present, this blueshift increases the optical coupling into the ring, which increases the carrier generation in the ring. The higher carrier generation in turn causes

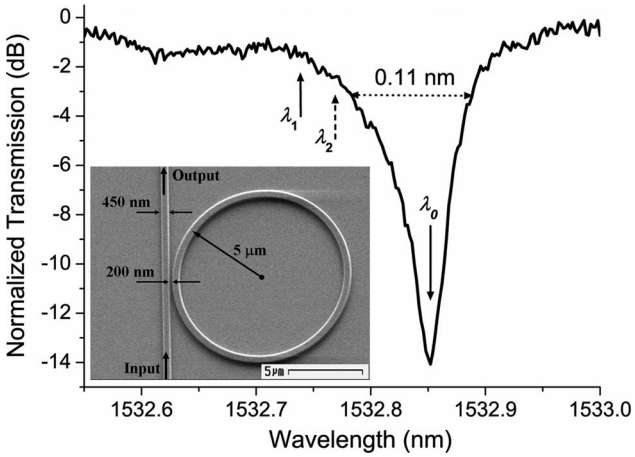

Fig. 1. Transmission spectrum of the ring resonator. Resonant wavelength λ_0 and the wavelengths used in the following bistability measurements, λ_1 and λ_2, are marked by arrows on the spectrum. Inset, top-view scanning-electron microscopy image of the ring resonator.

0146-9592/06/030341-3/$15.00

more blueshift of the resonance. This positive feedback process occurs until the blueshift induced by the input power is large enough that the wavelength of the input pulses becomes longer than the resonant wavelength of the ring. At this point, the previous positive feedback effect becomes a negative feedback effect, and the blueshifting process can be stabilized.

To demonstrate the bistability effect, we measure the transfer function (output power versus input power) of the ring resonator, which shows a hysteresis loop with input power higher than 3 mW. We use 4 ns optical pulses in the experiment. The width of the pulse is longer than the ~0.5 ns long carrier lifetime[4] to ensure that the carrier generation process reaches its steady state before the end of the pulses and is much shorter than the rise time of the thermal effect in the resonator, which is ~1 μs. The solid curves in Fig. 2 show the transfer function when input wavelength λ_1 is detuned from resonance as $\Delta\lambda_1=\lambda_1-\lambda_0=-0.11$ nm. These two curves show the output power when the input power is increasing and decreasing. One can see a sharp transition of output power when the ring resonator changes from the out-of-resonance (high output power) state to the on-resonance (low output power) state. This transition happens at two different input powers: P_1 (input power-increasing) and P_2 (input power-decreasing), forming a hysteresis loop. For the same input power of 6.2 mW, the output power of the ring resonator can be very different, depending on whether the pulse follows low input power (point A) or high input power (point B). To reach point A, one needs to increase input power from 0 to 6.2 mW, which is done by use of a single square pulse with 6.2-mW peak power, as shown in Fig. 3(a). Since the resonator is out of resonance before the pulse arrives, a small percentage of input power is coupled into the ring but is not sufficient to trigger positive feedback of the resonance blueshift. Therefore the resonator remains out of resonance as the pulse passes and the output power is high, as shown in Fig. 3(b). From Fig. 2, one can see that the input power required for triggering the blueshift of resonance, which will be referred to as the switching power, is $P_1\approx 9.5$ mW. To reach point B on the curve, one needs to have the input power decreased from a value higher than P_1. To achieve that, another high-power pulse (the leading pulse), whose wavelength is at the shorter-wavelength edge of another resonance of the ring, is sent to the waveguide immediately before the main pulse to be measured [see the lighter curve in Fig. 3(c)]. This leading pulse blueshifts the resonances of the ring. Therefore the resonator is on resonance before the main pulse with 6.2 mW peak power arrives [the darker curve in Fig. 3(c)], and most of the input power is coupled into the ring. The optical power coupled into the ring generates enough carriers to keep the resonance shifted, such that the resonator is kept on resonance and the output power is low, as shown in Fig. 3(d). From Fig. 2, one can see that the minimal power required to keep the resonator on resonance (the holding power) is $P_2\approx 5.5$ mW. The foregoing analysis shows that the state of a ring resonator depends on the previous state as well as on the current input, forming the basis for building sequential logic on silicon for applications such as all-optical routing.

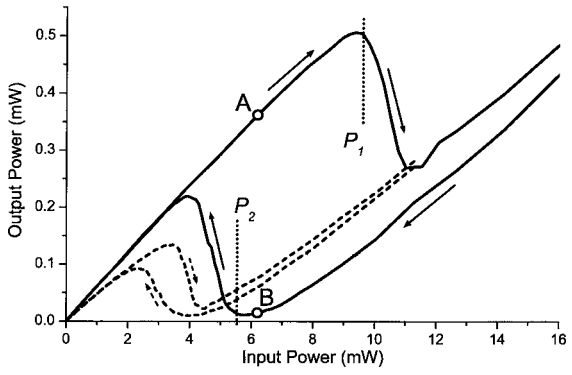

Fig. 2. Transfer function of the ring resonator with wavelength detuning of $\Delta\lambda_1=-0.11$ nm (solid curves) and $\Delta\lambda_2=-0.08$ nm (dashed curves), showing the bistability effect.

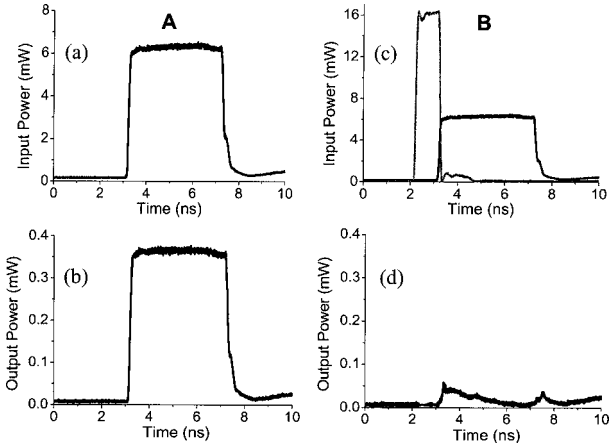

Fig. 3. Waveforms of input and output pulses for obtaining points A and B on the transfer function curves in Fig. 2. (a) Input pulse for obtaining point A. (b) Output pulse for the input shown in (a). (c) Input pulses for obtaining point B. The lighter curve shows the leading pulse, and the darker curve shows the main pulse, which is identical to the input pulse shown in (b). (d) Output pulse for the input shown in (c).

The shapes of the hysteresis curves agree with a theoretical analysis of nonlinear fiber ring resonators,[11] despite the fact that the type of nonlinearity involved is different. As the analysis shows, the difference between P_1 and P_2 decreases as the detuning from resonance λ_0 is reduced.[12] The dashed curves in Fig. 2 show the transfer function with detuning $\Delta\lambda_2=\lambda_2-\lambda_0=-0.08$ nm. One can see that the width of the hysteresis loop is much smaller.

The TPA of light in the resonator generates not only free carriers but also heat in the resonator, which results in changes in the temperature and refractive index of the silicon resonator. Here we show a quantitative comparison between the free-carrier effect and the thermal effect. Assuming the absorbed optical power that is due to TPA is P_A, the density of the generated electron–hole pair is determined by the equation

$$\frac{dN}{dt} + \frac{N}{\tau_c} = \frac{P_A}{2h\nu V}, \quad (1)$$

where N is the electron–hole pair's density, τ_c is the carrier lifetime, $h\nu = 1.28 \times 10^{-19}$ J is the photon energy, and V is the volume of the ring cavity. The refractive index of silicon changes with carrier density as $\Delta n_c = \kappa_c N$, where $\kappa_c = 1.35 \times 10^{-21}$ cm^3 (Refs. 13 and 14) for N of the order of 10^{17} cm^{-3}. Since both TPA and carrier recombination are phonon-assisted processes, all the absorbed energy is eventually converted to thermal energy, and the temperature shift can be obtained from the equation

$$\frac{d\Delta T}{dt} + \frac{\Delta T}{\tau_\theta} = -\frac{P_A}{\rho C V}, \quad (2)$$

where $\tau_\theta \sim 1$ μs (Ref. 7) is the thermal dissipation time, $\rho = 2.3 \times 10^{-3}$ kg/cm^3 is the density of silicon, and $C = 705$ J/(kg·K) is the thermal capacity. The refractive index of silicon changes with temperature as $\Delta n_\theta = \kappa_\theta \Delta T$, where $\kappa_\theta = 1.86 \times 10^{-4}$ K^{-1}.[15] In steady state, the ratio between the temperature-induced index change and the carrier-induced index change is

$$\frac{\Delta n_\theta}{\Delta n_c} = \frac{2h\nu\kappa_\theta\tau_\theta}{\rho C \kappa_c \tau_c} \approx -0.022\frac{\tau_\theta}{\tau_c}, \quad (3)$$

where $\tau_c = 0.5$ ns, $\tau_\theta \sim 1$ μs, and $\Delta n_\theta / \Delta n_c \sim -44$. Therefore, with cw optical input, the thermal nonlinear effect dominates the carrier nonlinear effect. We have observed optical bistability based on the thermal effect in a silicon ring resonator with cw optical power of less than 1 mW.[7] When the optical input is a nanosecond pulse with pulse width T satisfying $\tau_c \ll T \ll \tau_\theta$,

$$\frac{\Delta n_\theta}{\Delta n_c} = \frac{2h\nu\kappa_\theta T}{\rho C \kappa_c \tau_c} \approx -0.022\frac{T}{\tau_c}. \quad (4)$$

Therefore the carrier's nonlinear effect becomes higher than the thermal nonlinear effect when T is smaller than $46\tau_c = 23$ ns.

The thermal effect shown above affects carrier-based bistability. In the experiment, when the ring resonator is in state B as shown in Fig. 2, heat is generated in the ring resonator as a result of high optical coupling to the ring, which results in a temperature increase and a redshift of the resonance. As the wavelength and the power of the optical input are fixed, the redshift of the resonance increases the detuning and therefore increases the required holding power P_2. Once P_2 becomes higher than the input power, the device jumps to state A. This phenomenon prevents the carrier-induced bistability from operating at steady state. By using a longer main pulse in the experiment, we observe that the resonator can be held in state B for less than 10 ns before it starts to change back to state A. To minimize the thermal effect, strain in the silicon waveguide could be used,[16] which can be introduced during the fabrication process by, for example, controlling the overcladding deposition conditions.[17] The introduced strain induces a decrease of the refractive index with the increase of temperature, which can counterbalance the thermo-optical effect, leading to steady-state bistability from the carrier effect.

In conclusion, we have shown experimentally carrier-induced optical bistability in a silicon ring resonator with an optical power of less than 10 mW. For the same optical input power, the transmission of the resonator can be vastly different, depending on the previous state of the resonator. This effect can be used in applications such as logic for all-optical routing.

M. Lipson's e-mail address is lipson @ece.cornell.edu.

References

1. O. Boyraz and B. Jalali, Opt. Express **12**, 5269 (2004).
2. A. Liu, R. Jones, L. Liao, D. Samara-Rubio, D. Rubin, O. Cohen, R. Nicolaescu, and M. Paniccla, Nature **427**, 615 (2004).
3. Q. Xu, B. Schmidt, S. Pradhan, and M. Lipson, Nature **435**, 325 (2005).
4. V. R. Almeida, C. A. Barrios, R. R. Panepucci, and M. Lipson, Nature **431**, 1081 (2004).
5. T. A. Ibrahim, R. Grover, L. C. Kuo, S. Kanakaraju, L. C. Calhoun, and P. T. Ho, IEEE Photon. Technol. Lett. **15**, 1422 (2003).
6. T. A. Ibrahim, K. Amarnath, L. C. Kuo, R. Grover, V. Van, and P. T. Ho, Opt. Lett. **29**, 2779 (2004).
7. V. R. Almeida and M. Lipson, Opt. Lett. **29**, 2387 (2004).
8. M. N. T. Tanabe, A. Shinya, S. Mitsugi, and E. Kuramochi, in *Conference on Lasers and Electro-Optics (CLEO)* (Optical Society of America, 2005), paper QPDA5.
9. V. R. Almeida, R. R. Panepucci, and M. Lipson, Opt. Lett. **28**, 1302 (2003).
10. M. Dinu, F. Quochi, and H. Garcia, Appl. Phys. Lett. **82**, 2954 (2003).
11. K. Ogusu, IEEE J. Quantum Electron. **32**, 1537 (1996).
12. P. E. Barclay, K. Srinivasan, and O. Fainter, Opt. Express **13**, 801 (2005).
13. R. A. Soref and B. R. Bennett, IEEE J. Quantum Electron. **QE-23**, 123 (1987).
14. C. A. Barrios, V. R. Almeida, R. Panepucci, and M. Lipson, J. Lightwave Technol. **21**, 2332 (2003).
15. G. Cocorullo and I. Rendina, Electron. Lett. **28**, 83 (1992).
16. S. M. Weiss, M. Molinari, and P. M. Fauchet, Appl. Phys. Lett. **83**, 1980 (2003).
17. P. Cheben, D.-X. Xu, S. Janz, and A. Delage, in Proc. SPIE **5117**, 147 (2003).